Hindawi Publishing Corporation
Advances in Astronomy
Volume 2015, Article ID 192383, 16 pages
http://dx.doi.org/10.1155/2015/192383

*Review Article*

# Reverse Shock Emission in Gamma-Ray Bursts Revisited

**He Gao and Peter Mészáros**

*Department of Astronomy and Astrophysics, Department of Physics, Center for Particle and Gravitational Astrophysics, Institute for Gravitation and the Cosmos, 525 Davey Lab, Pennsylvania State University, University Park, PA 16802, USA*

Correspondence should be addressed to He Gao; hug18@psu.edu

Received 26 November 2014; Accepted 7 April 2015

Academic Editor: Valery Nakariakov



A generic synchrotron external shock model is the widely preferred paradigm used to interpret the broadband afterglow data of gamma-ray bursts (GRBs), including predicted observable signatures from a reverse shock which have been confirmed by observations. Investigations of the nature of the reverse shock emission can provide valuable insights into the intrinsic properties of the GRB ejecta. Here we briefly review the standard and the extended models of the reverse shock emission, discussing the connection between the theory and observations, including the implications of the latest observational advances.

## 1. Introduction

Gamma-ray bursts (GRBs), which are the most extreme explosive events in the universe, generally present two phenomenological emission phases: an initial prompt $\gamma$-ray emission and a longer-lived broadband afterglow emission. Regardless of the nature of the progenitor and the central engine, the radiation of the GRBs is believed to be caused by the dissipation of the kinetic energy of a relativistic jet which is beamed towards Earth (for reviews, see [1–5]). Although the detailed physics of the prompt $\gamma$-ray emission is still uncertain, mainly owing to the poorly understanding composition of the GRB jet (e.g., the degree of magnetization) [6], a generic synchrotron external shock model is the most widely accepted paradigm for interpreting the broadband afterglow data [7–12].

The external shock model is based on a relativistic blastwave theory that describes the interaction between the GRB jet (i.e., the ejecta) and the circumburst medium (for detailed reviews, see [13]). During the interaction, two shocks naturally develop. A long-lived forward shock sweeps up the ambient medium, which gives rise to the long-term broadband afterglow; and a short-lived reverse shock propagates into the GRB ejecta, which can give rise to a short-term optical/IR flash and a radio flare. In the pre-*Swift* era, the forward shock signal was found to successfully represent a large array of late-time afterglow data [14–21], although moderate revisions are sometimes required [13] for the more complicated afterglow behaviors [22–26]. After the launch of NASA's dedicated GRB mission *Swift* [27], unprecedented new information about GRB afterglows was revealed [28–33], especially in the early phases, thanks mainly to the rapid slewing and precise localization capability of its on-board X-Ray Telescope (XRT) [34]. It was found that a number of physical processes are needed to shape the observed lightcurves [30, 31], including, for example, the suggestion that the X-ray afterglow is a superposition of the conventional external shock component and a radiation component that is related to the late central engine activity [4, 29, 30, 35–46]. In any case, the external forward shock still remains the basic theoretical framework to interpret the broadband afterglow signals. It is elegant in its simplicity, since it invokes a limit number of model parameters (e.g., the total energy of the system, the ambient density, and its profile) and has well defined predicted spectral and temporal properties. However, it lacks the ability to study some detailed features of the GRB ejecta, such as the composition, since its radiation comes from the shocked medium rather than the ejecta materials.

The reverse shock, on the other hand, should heat the GRB ejecta within a short period of time, contributing another important aspect to the external shock emission signature. The hydrodynamics of reverse shock propagation in a matter-dominated shell and its corresponding radiation features were studied in great detail [9, 10, 47, 48] prior to

the expected signals being discovered. In the pre-*Swift* era, some cases with very early optical flashes (e.g., GRB 990123 [22]; GRB 021004 [25]; GRB 021211 [26, 49]) or early radio flares [50] were detected, which generally agreed well with the predicted reverse shock emission [51–63].

However, there are also some observations which challenge the simple reverse shock prediction. For instance, the early optical emission of GRB 030418 [64] does not agree with the predicted reverse shock behavior; furthermore, rapid optical follow-up observations for some bursts reveal the so-called "optical flash problem," for example, upper limits of 15 mag were established for specific observed bursts, instead of detecting the expected reverse shock emission [65–68]. In order to better interpret the observational results, the simple reverse shock model was extended to accommodate more realistic conditions than what was initially assumed. For example, the ambient medium might be a stellar wind (or in general have a profile $n \propto r^{-k}$) rather than being a uniform interstellar medium [69–72]; the reverse shock propagation speed might be semirelativistic instead of ultrarelativistic or nonrelativistic [62]; the GRB ejecta might be magnetized, which could enhance the signal when the magnetization is moderate, or completely suppress the signal when magnetization degree is large enough [73–78]; the GRB outflow may carry a good fraction of electron-position pairs or neutrons which could alter the early afterglow behavior [79, 80]; considering a more complicated stratification profile of the ejecta, for example, with a nonuniform Lorentz factor, luminosity, and density, the reverse shock emission could have a richer set of features, including being able to reproduce the canonical X-ray lightcurves as observed by *Swift* as long as the forward shock emission is suppressed [81–86]. Beside these model modifications, some new signatures for reverse shock were also proposed, such as sub-GeV photon flashes and high energy neutrino emission [87, 88] and early X-ray and gamma-ray emission from synchrotron self-Compton (SSC) in the reverse shock region or cross inverse Compton (IC) between the electrons and photons from the forward shock and reverse shock [89, 90], or a polarization signature that offers the possibility to diagnose the structure of the magnetic fields in the GRB ejecta.

Before the launch of *Swift*, the observational data was not ample or detailed enough to comprehensively test these reverse shock models or to study the ejecta properties through the reverse shock signatures. A good sample of early afterglow lightcurves which would allow a detailed study of GRB reverse shocks was one of the expectations from the *Swift* mission [1, 27]. After ten years of successful operation of *Swift*, it is now of great interest to revisit this problem and to see how much progress has been made.

The structure of this review is as follows: we first summarize the models for the reverse shock emission, including the standard synchrotron external shock model in Section 2, and discuss the extended models in Section 3. In Section 4, we illustrate how to identify in practice the reverse shock signals present in the observational data and how to use such signals to study the GRB ejecta properties. The current observational results and their implications are collected in Section 5. We conclude with a brief discussion of the prospects for future reverse shock studies.

## 2. Standard Modeling of the Reverse Shock Emission

*2.1. Model Description.* Consider a uniform relativistic coasting shell with rest mass $M_0$, energy $E$, initial Lorentz factor $\eta = E/M_0c^2$, and observed width $\Delta$, expanding into the circumburst medium (CBM) described by a density profile $n(r) = Ar^{-k}, 0 \le k < 4$. A pair of shocks will develop, namely, a forward shock propagating into the medium and a reverse shock propagating into the shell. The two shocks and the contact discontinuity separate the system into four regions: (1) the unshocked CBM (called region 1 hereafter), (2) the shocked CBM (region 2), (3) the shocked shell (region 3), and (4) the unshocked shell (region 4). Synchrotron emission is expected from regions 2 and 3, since electrons are accelerated at the shock fronts via the 1st-order Fermi acceleration mechanism and magnetic fields are believed to be generated behind the shocks due to plasma instabilities (for forward shock) [93] or shock compression amplification of the magnetic field carried by the central engine (for reverse shock).

An evaluation of the hydrodynamical and thermodynamical quantities for the regions 2 and 3, namely, $\gamma_i, n_i, p_i$ and $e_i$ (bulk Lorentz factor, particle number density, pressure, and internal energy density, with $i$ denoting the region number), allows one to straightforwardly calculate the instantaneous synchrotron spectrum at a given epoch, as well as the flux evolution in time (the lightcurve) for a given observed frequency. In doing this, it is customary to introduce parametrizations for the microscopic processes, such as the fractions of the shock energy that go into the electrons and into magnetic fields ($\epsilon_e$ and $\epsilon_B$) and the electron spectral index ($p$). Reference [13] gives detailed examples about such calculations and provides a complete reference for all the analytical synchrotron external shock afterglow models by deriving the temporal and spectral indices of all the models in all spectral regimes. In order to review the reverse shock related features, we give here a brief summary of the dynamical properties of region 3 for various models.

In general, region 3 will evolve through two different phases, that is, before the reverse shock crossing the shell (at $T_x$) and after the reverse shock crossing. The dynamical solution depends on the relativistic nature of the reverse shock, which can be characterized by the dimensionless parameter $\xi \equiv (l/\Delta)^{1/2}\eta^{-(4-k)/(3-k)}$ [47, 72], where $l = ((3-k)E/4\pi Am_pc^2)^{1/(3-k)}$ is the Sedov length (at which the swept-up medium's rest-mass energy equals the initial energy $E$ of the shell). If $\xi \ll 1$, the reverse shock is ultrarelativistic (thick shell regime), while if $\xi \gg 1$, the reverse shock is Newtonian (thin shell regime). Between these two extreme limits, the reverse shock can be considered semirelativistic when $\xi$ is of the order of unity [62]. Combined with the different (generic) types of CBM, that is, constant density interstellar medium

(ISM) model ($k = 0$), stellar wind model ($k = 2$), and general stratified wind model ($0 \le k < 4$), seven different regimes have been studied in the literature [47, 54, 62, 69–72]. These are (1) thick shell ISM ($\xi \ll 1, n_1 \propto r^0$); (2) thin shell ISM ($\xi \gg 1, n_1 \propto r^0$); (3) thick shell stellar wind ($\xi \ll 1, n_1 \propto r^{-2}$); (4) thin shell stellar wind ($\xi \gg 1, n_1 \propto r^{-2}$); (5) thick shell general stratified wind ($\xi \ll 1, n_1 \propto r^{-k}$); (6) thin shell general stratified wind ($\xi \gg 1, n_1 \propto r^{-k}$); (7) semirelativistic reverse shock ISM ($\xi \sim 1, n_1 \propto r^0$). Below, we summarize the results in the literature for these different regimes.

*(1) Thick Shell ISM ($\xi \ll 1, n_1 \propto r^0$) [47, 54].* In this case, the reverse shock crossing time can be estimated as $T_x = \Delta/c$, which is independent of the CBM (applied to all thick shell regimes below). Before $T_x$, the dynamic variables of region 3 in terms of the observer time $t = r/2c\gamma_3^2$ are

$$\begin{aligned}
\gamma_3 &= \left(\frac{l}{\Delta}\right)^{3/8}\left(\frac{4ct}{\Delta}\right),\\
n_3 &= \frac{8\gamma_3^3 n_1}{\eta} \propto t^{-3/4},\\
p_3 &= \frac{4\gamma_3^2 n_1 m_p c^2}{3} \propto t^{-1/2},\\
N_e &= N_0\frac{ct}{\Delta},
\end{aligned} \tag{1}$$

where $N_0 = E/\eta m_p c^2$ is the total number of electrons in the shell. Since the shocked regions (regions 2 and 3) should be extremely hot, the energy density term is degenerate with the pressure term as $e_3 = 3p_3$.

After $T_x$, the profile of the shocked medium in region 2 begins to approach the Blandford-McKee (BM) self-similar solution [137, 138]. Since region 3 is located not too far behind region 2, it should roughly fit the BM solution, which is verified numerically as long as the relativistic reverse shock can heat the shell to a relativistic temperature [139]. The BM scaling thus can be applied to the evolution of the shocked shell:

$$\begin{aligned}
\gamma_3 &= \gamma_3(T_x)\left(\frac{t}{T_x}\right)^{-7/16},\\
n_3 &= n_3(T_x)\left(\frac{t}{T_x}\right)^{-13/16},\\
p_3 &= p_3(T_x)\left(\frac{t}{T_x}\right)^{-13/12},\\
N_3 &= N_0.
\end{aligned} \tag{2}$$

Note that the number of the shocked electrons is constant after the shock crossing since no electrons are newly shocked.

*(2) Thin Shell ISM ($\xi \gg 1, n_1 \propto r^0$) [47, 54].* In a thin shell case, the reverse shock is too weak to decelerate the shell effectively. $T_x$ can be estimated by the deceleration time of the ejecta (applied to all thin shell regimes below):

$$T_x \simeq t_{\rm dec} = \left[\frac{(3-k)E}{2^{4-k}\pi A m_p \Gamma_0^{8-2k} c^{5-k}}\right]^{1/(3-k)}. \tag{3}$$

Before $T_x$, the scaling for the dynamic variables of region 3 is given by

$$\begin{aligned}
\gamma_3 &= \eta,\\
n_3 &= 7n_1\eta^2\left(\frac{t}{T_x}\right)^{-3},\\
p_3 &= \frac{4\eta^2 n_1 m_p c^2}{3},\\
N_3 &= N_0\left(\frac{t}{T_x}\right)^{3/2}.
\end{aligned} \tag{4}$$

After $T_x$, the Lorentz factor of the shocked shell may be assumed to have a general power-law decay behavior $\gamma_3 \propto r^{-g}$ [52, 53]. The dynamical behavior in region 3 may be expressed through the scaling-laws:

$$\begin{aligned}
\gamma_3 &\propto t^{-g/(1+2g)},\\
n_3 &\propto t^{-6(3+g)/7(1+2g)},\\
p_3 &\propto t^{-8(3+g)/7(1+2g)},\\
r &\propto t^{1/(1+2g)},\\
N_{e,3} &\propto t^0.
\end{aligned} \tag{5}$$

For the ISM case, numerical studies showed that the scaling with $g \sim 2$ fits the evolution [53]; for example,

$$\begin{aligned}
\gamma_3 &= \gamma_3(T_x)\left(\frac{t}{T_x}\right)^{-2/5},\\
n_3 &= n_3(T_x)\left(\frac{t}{T_x}\right)^{-6/7},\\
p_3 &= p_3(T_x)\left(\frac{t}{T_x}\right)^{-8/7},\\
N_3 &= N_0.
\end{aligned} \tag{6}$$

*(3) Thick Shell Stellar Wind ($\xi \ll 1, n_1 \propto r^{-2}$) [69, 70].* Similar to regime 1, before $T_x$, we have

$$\begin{aligned}
\gamma_3 &= \frac{1}{\sqrt{2}}\left(\frac{l}{\Delta}\right)^{1/4},\\
n_3 &= \frac{8\sqrt{2}A}{\eta l^{1/4}\Delta^{7/4}}\left(\frac{t}{T_x}\right)^{-2},\\
p_3 &= \frac{8Am_p c^2}{3l^{1/2}\Delta^{3/2}}\left(\frac{t}{T_x}\right)^{-2},\\
N_3 &= N_0\frac{t}{T_x}.
\end{aligned} \tag{7}$$

After $T_x$, assuming a BM self-similar adiabatic solution for the evolution of the shocked shell [53], the relevant hydrodynamic variables are given by

$$\begin{aligned} \gamma_3 &= \gamma_3(T_x)\left(\frac{t}{T_x}\right)^{-3/8}, \\ n_3 &= n_3(T_x)\left(\frac{t}{T_x}\right)^{-9/8}, \\ p_3 &= p_3(T_x)\left(\frac{t}{T_x}\right)^{-3/2}, \\ N_3 &= N_0. \end{aligned} \tag{8}$$

*(4) Thin Shell Stellar Wind ($\xi \gg 1, n_1 \propto r^{-2}$) [71].* In this case, the evolution of the hydrodynamic variables before the time $T_x$ is

$$\begin{aligned} \gamma_3 &= \eta, \\ n_3 &= \frac{7A\eta^6}{l^2}\left(\frac{t}{T_x}\right)^{-3}, \\ p_3 &= \frac{4Am_pc^2\eta^6}{3l^2}\left(\frac{t}{T_x}\right)^{-2}, \\ N_3 &= N_0\left(\frac{t}{T_x}\right)^{1/2}. \end{aligned} \tag{9}$$

After the reverse shock crosses the shell, the scaling law for regime 2 still applies, except $g = 1$; namely,

$$\begin{aligned} \gamma_3 &= \gamma_3(T_x)\left(\frac{t}{T_x}\right)^{-1/3}, \\ n_3 &= n_3(T_x)\left(\frac{t}{T_x}\right)^{-8/7}, \\ p_3 &= p_3(T_x)\left(\frac{t}{T_x}\right)^{-32/21}, \\ N &= N_0. \end{aligned} \tag{10}$$

*(5) Thick Shell General Stratified Wind ($\xi \ll 1, n_1 \propto r^{-k}$) [72].* Before the reverse shock crosses the shell, the hydrodynamical evolution of the reverse shock can be characterized by

$$\begin{aligned} \gamma_3 &= \gamma_3(T_x)\left(\frac{t}{T_x}\right)^{-(2-k)/2(4-k)}, \\ n_3 &= n_3(T_x)\left(\frac{t}{T_x}\right)^{-(6+k)/2(4-k)}, \\ p_3 &= p_3(T_x)\left(\frac{t}{T_x}\right)^{-(2+k)/(4-k)}, \\ N_3 &= N_0\frac{t}{T_x}, \end{aligned} \tag{11}$$

where

$$\begin{aligned} \gamma_3(T_x) &= \left[2^k(3-k)(4-k)^{2-k}\right]^{-1/2(4-k)} \\ &\quad\cdot\left(\frac{l}{\Delta}\right)^{(3-k)/2(4-k)}, \\ n_3(T_x) &= \left[2^{24-k}(3-k)^{2k-3}(4-k)^{-(6+k)}\right]^{1/2(4-k)} \\ &\quad\cdot\frac{A}{\eta}\left(l^{(3-2k)(3-k)}\Delta^{k-9}\right)^{1/2(4-k)}, \\ \gamma_{34}(T_x) &= \left[2^{3k-8}(3-k)(4-k)^{2-k}\right]^{1/2(4-k)} \\ &\quad\cdot\eta\left(\frac{l}{\Delta}\right)^{-(3-k)/2(4-k)}, \\ p_3(T_x) &= 3\gamma_{34}(T_x)n_3(T_x)m_pc^2. \end{aligned} \tag{12}$$

After the reverse shock crosses the shell, again with a BM self-similar solution, one gets $\gamma_3 \propto r^{(2k-7)/2}$, $p_3 \propto r^{(4k-26)/3}$, $n_3 \propto r^{(2k-13)/2}$ and $t \propto r/\gamma_3^2 c$. Thus, the hydrodynamic evolution of the reverse shock after crossing the shell is characterized by

$$\begin{aligned} \gamma_3 &= \gamma_3(T_x)\left(\frac{t}{T_x}\right)^{(2k-7)/4(4-k)}, \\ n_3 &= n_3(T_x)\left(\frac{t}{T_x}\right)^{(2k-13)/4(4-k)}, \\ p_3 &= p_3(T_x)\left(\frac{t}{T_x}\right)^{(2k-13)/3(4-k)}, \\ N_3 &= N_0. \end{aligned} \tag{13}$$

*(6) Thin Shell General Stratified Wind ($\xi \gg 1, n_1 \propto r^{-k}$) [72].* In this case, before $T_x$, the hydrodynamic evolution of the reverse shock can be characterized by

$$\begin{aligned} \gamma_3 &= \eta, \\ n_3 &= n_3(T_x)\left(\frac{t}{T_x}\right)^{-3}, \\ p_3 &= p_3(T_x)\left(\frac{t}{T_x}\right)^{-k}, \\ N_3 &= N_0\left(\frac{t}{T_x}\right)^{(3-k)/2}, \end{aligned} \tag{14}$$

where

$$n_3(T_x) = \left[\frac{2^9 7^{6-k}}{3^6 (3-k)^{6-k}}\right]^{1/(3-k)} A^{1-k}\eta^{6/(3-k)},$$
$$\gamma_{34,\Delta} = 1 + \frac{9(3-k)^2}{98}, \quad (15)$$
$$p_3(T_x) = 3(\gamma_{34}(T_x) - 1) n_3(T_x) m_p c^2.$$

After the reverse shock crosses the shell, the scaling law for regime 2 should be still relevant, except that the value of $g$ has not been studied in detail.

*(7) Mild Relativistic Reverse Shock ISM ($\xi \sim 1$, $n_1 \propto r^0$) [62].* In this case, a simple analytical solution is no longer achievable. The nature of the reverse shock is determined by $\xi$ and another parameter $a$, which is the ratio of the Lorentz factor of the shocked matter to $\eta$,

$$a \equiv \frac{\gamma_3}{\eta}. \quad (16)$$

Here $a$ can be derived directly from the relativistic jump conditions [47]:

$$\left(\frac{12}{\xi^3} - 1\right) a^4 + 0.5a^3 + a^2 + 0.5a - 1 = 0. \quad (17)$$

The reverse shock reaches the back of the shell at

$$T_x = \frac{\Delta}{c}\left(1 + 0.5\mathcal{N}_t \xi^{3/2}\right), \quad (18)$$

where $\mathcal{N}_t = 1.4$ is a numerical correction factor to the analytic estimates [62]. At this stage,

$$p_r = \frac{4}{3} a^2 \eta^2 n_1 m_p c^2;$$
$$n_r = \xi^3 n_1 \eta^2 \left(\frac{2(a + 1/a)}{3} + 1\right). \quad (19)$$

When $t < T_x$, the dynamical variables of region 3 can be determined by parameterizing all the quantities according to the fraction of the reverse shock crossing the shell, $f$:

$$\Delta(f) \propto E(f) \propto f,$$
$$\xi(f) \propto f^{-1/3},$$
$$r(f) \propto f^{1/2}, \quad (20)$$
$$t(f) \propto f\left(1 + 0.5\mathcal{N}_t \xi(f)^{3/2}\right).$$

At $t > T_x$, the hydrodynamical evolution becomes almost independent of $\xi$ [53]; therefore, the solutions for the dynamic variables of region 3 become the same as in regime 2.

*2.2. Emission Evolution.* The instantaneous synchrotron spectrum at a given epoch can be described with three characteristic frequencies $\nu_a$ (self-absorption frequency), $\nu_m$, and $\nu_c$ (the cooling frequency) and the peak synchrotron flux density $F_{\nu,\max}$ [11]. Based on the dynamical solution for specific situations, one can calculate the temporal evolution of these characteristic parameters and then determine the flux evolution in time (the lightcurve) for a given observed frequency. Since the reverse shock emission is expected to be prominent in the optical band at early stage, here we give a brief description for the morphology of early optical afterglow lightcurves.

It is shown that for reasonable parameter spaces, shortly after (or even during) the prompt emission phase, both forward shock and reverse shock emissions would enter into the "slow cooling" regime ($\nu_c < \nu_m$) [11, 58]. In the following, we will take slow cooling for both reverse and forward shock emissions, so that the shape of the lightcurve essentially depends on the relation between $\nu_m^{r,f}$ and $\nu_{\rm opt}$, where the superscripts $r$ and $f$ represent reverse and forward shock, respectively.

For thin shell case, the evolution of $\nu_m^{r,f}$ reads

$$\nu_m^f \propto t^0 \quad (t < T_x),$$
$$\nu_m^f \propto t^{-3/2} \quad (t > T_x),$$
$$\nu_m^r \propto t^6 \quad (t < T_x), \quad (21)$$
$$\nu_m^r \propto t^{-3/2} \quad (t > T_x).$$

As shown in Figure 1(a), when $\nu_m^{r,f}(T_x)$ is larger than $\nu_{\rm opt}$, $\nu_m^{r,f}$ would cross the optical band once for the forward shock (at $t_f$) and twice for the reverse shock (at $t_{r,1}$ and $t_{r,2}$). In this case, we have (shown in Figure 1(b))

$$F_\nu^f \propto t^3 \quad (t < T_x),$$
$$F_\nu^f \propto t^{1/2} \quad (T_x < t < t_f),$$
$$F_\nu^f \propto t^{-3(p-1)/4} \quad (t > t_f),$$
$$F_\nu^r \propto t^{(6p-3)/2} \quad (t < t_{r,1}), \quad (22)$$
$$F_\nu^r \propto t^{-1/2} \quad (t_{r,1} < t < t_{r,2}),$$
$$F_\nu^r \propto t^{-(27p+7)/35} \quad (t > t_{r,2}).$$

When $\nu_m^{r,f}(T_x)$ is smaller than $\nu_{\rm opt}$, there is no $\nu_m$ crossing and the lightcurves for both shocks peak at $T_x$. In this case, we have

$$F_\nu^f \propto t^3 \quad (t < T_x),$$
$$F_\nu^f \propto t^{-3(p-1)/4} \quad (t > T_x),$$
$$F_\nu^r \propto t^{(6p-3)/2} \quad (t < T_x), \quad (23)$$
$$F_\nu^r \propto t^{-(27p+7)/35} \quad (t > T_x).$$

Depending on their shapes and relative relations between the forward shock and reverse shock emission, the early optical

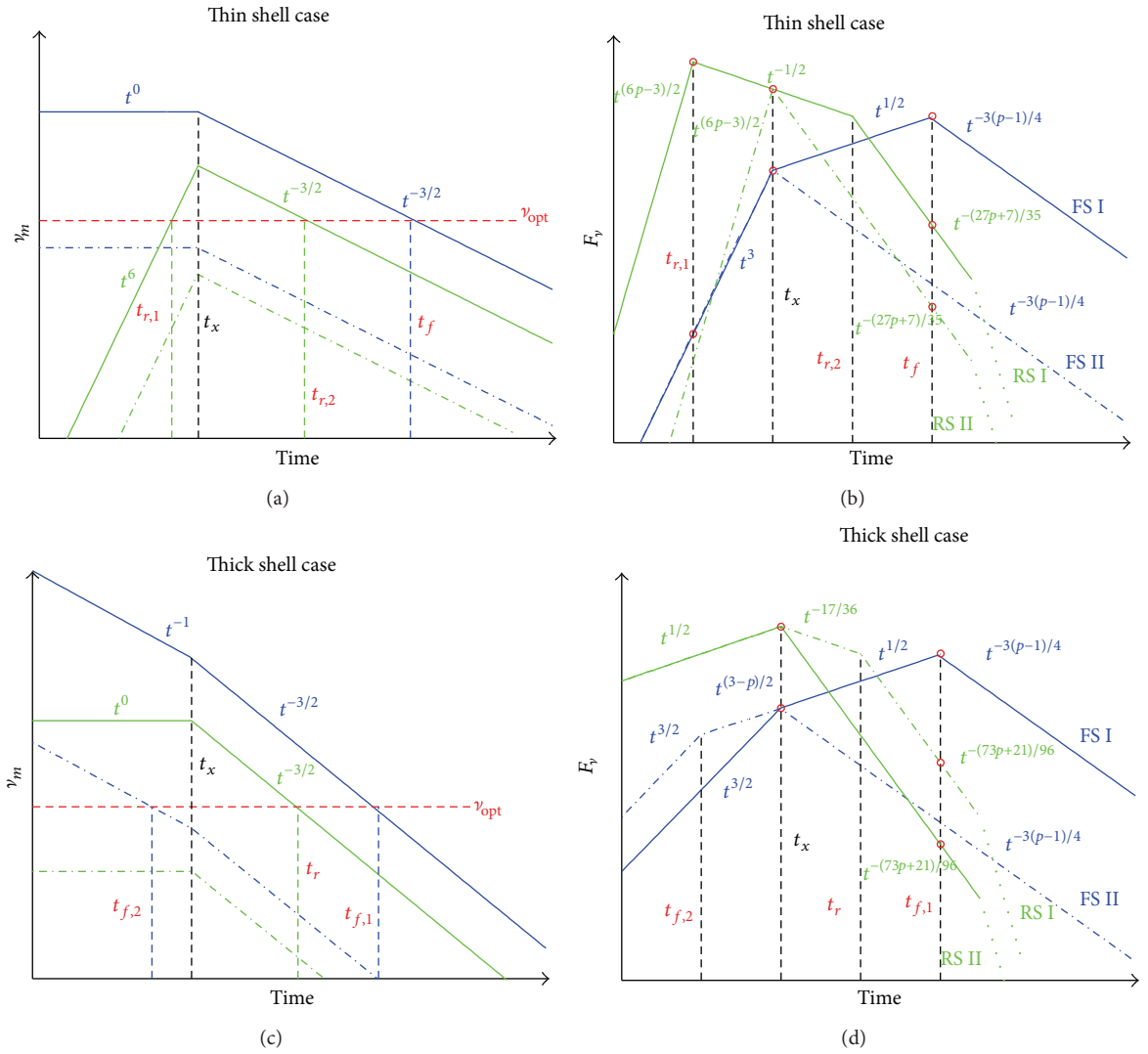


FIGURE 1: Illustration of the $\nu_m$ evolution ((a), (c)) and optical lightcurves ((b), (d)) for both forward shock (blue lines) and reverse shock (green lines) emission, from [91]. Red circles on lightcurve indicate the points for comparison in order to categorize the lightcurve types [91].

lightcurves could be distributed into different morphological types; we will discuss this in detail in Section 4.1.

For thick shell case, the evolution of $\nu_m^{r,f}$ reads (shown in Figure 1(c))

$$\begin{aligned}
&\nu_m^f \propto t^{-1} \quad (t < T_x),\\
&\nu_m^f \propto t^{-3/2} \quad (t > T_x),\\
&\nu_m^r \propto t^{0} \quad (t < T_x),\\
&\nu_m^r \propto t^{-3/2} \quad (t > T_x).
\end{aligned} \tag{24}$$

When $\nu_m^{r,f}(T_x)$ is larger than $\nu_{\rm opt}$, $\nu_m^{r,f}$ would cross the optical band once for both forward shock (at $t_{f,1}$) and reverse shock (at $t_r$). In this case, we have (shown in Figure 1(d))

$$\begin{aligned}
&F_\nu^f \propto t^{3/2} \quad (t < T_x),\\
&F_\nu^f \propto t^{1/2} \quad (T_x < t < t_f),\\
&F_\nu^f \propto t^{-3(p-1)/4} \quad (t > t_f),\\
&F_\nu^r \propto t^{1/2} \quad (t < T_x),\\
&F_\nu^r \propto t^{-17/36} \quad (T_x < t < t_r),\\
&F_\nu^r \propto t^{-(73p+21)/96} \quad (t > t_r).
\end{aligned} \tag{25}$$

When $\nu_m^{r,f}(T_x)$ is smaller than $\nu_{\rm opt}$, there is no $\nu_m$ crossing for reverse shock but there is one time crossing for forward shock (at $t_{f,2}$). In this case, we have

$$\begin{aligned}
&F_\nu^f \propto t^{3/2} \quad (t < t_{f,2}),\\
&F_\nu^f \propto t^{(3-p)/2} \quad (t_{f,2} < t < T_x),\\
&F_\nu^f \propto t^{-3(p-1)/4} \quad (t > T_x),
\end{aligned}$$

$$F_\nu^r \propto t^{1/2} \quad (t < T_x),$$
$$F_\nu^r \propto t^{-(73p+21)/96} \quad (t > T_x). \tag{26}$$

## 3. Extended Models of the Reverse Shock Emission

*3.1. Reverse Shock Emission from Magnetized GRB Ejecta.* It has been suggested that the GRB ejecta are likely to be magnetized (see [5] for a recent review). Although the degree of magnetization is still unknown, it is usually quantified through the parameter $\sigma$, the ratio of the electromagnetic energy flux to the kinetic energy flux. The existence of magnetic fields in the ejecta will influence at least two aspects of the reverse shock characteristics, that is, the hydrodynamical solutions for the shocked shell region and the reverse shock emission level.

Under ideal MHD conditions and with a more accurate approach to account for the modifications in the shock jump conditions when magnetic fields are involved, a rigorous analytical solution for the relativistic 90° shocks was carried out and several interesting conclusions were suggested [73]:

(i) A strong reverse shock still exists in the high-$\sigma$ regime, as long as the shock is relativistic. For typical GRB parameters, the reverse shock could form when $\sigma$ is as high as several tens or even hundreds, which is supported numerically by solving the one-dimensional Riemann problem for the deceleration of an arbitrarily magnetized relativistic flow [77].

(ii) The dynamical evolution of region 3 can be still categorized into the thick and thin shell regimes, except that the pivotal parameter to separate the two regimes now becomes $\sigma$. At larger $\sigma$-value, the thick shell regime greatly shrinks and the reverse shock emission peak is broadened in the thin shell regime due to the separation of the shock crossing radius and the deceleration radius. Such novel features could be useful for diagnosing the magnetization degree of GRB ejecta.

(iii) The reverse shock emission level should initially increase rapidly as $\sigma$ increases from below, until reaching a peak around $\sigma \sim 0.1$–1, and decreases steadily when $\sigma > 1$. The decrease of the emission level is caused not only because the reverse shock becomes weaker, but also because the total kinetic energy fraction in the flow gets smaller. Separate investigations of the reverse shock emission powered by mildly magnetized ($\sigma \sim 0.05$–1) GRB ejecta were also carried out numerically [140], and similar results were achieved. In that work [140], both ISM and stellar wind CBMs were considered, and it turns out that, before the reverse shock crosses the ejecta, the relevant R-band emission flux increases rapidly for the ISM medium case, but for the wind case it increases only slightly, which is similar to nonmagnetized scenario. Recently, multiband GRB afterglow lightcurves for magnetized ejecta have been calculated with high-resolution relativistic MHD simulations coupled with a radiative transfer code [75, 76], and it is suggested that, for typical parameters of the ejecta, the emission from the reverse shock peaks at magnetization values $\sigma \sim 0.01$–0.1 of the flow and that it is greatly suppressed for higher $\sigma$-values.

(iv) In the high $\sigma$-value regime, a sufficient magnetic energy has not yet been transferred to the ISM at the end of the reverse shock crossing, since the magnetic pressure behind the contact discontinuity balances the thermal pressure in the forward shock crossing. The leftover magnetic energy would eventually be injected into the blastwave or dissipate into radiation at some point and provide additional signatures to the afterglow lightcurve [73, 76].

*3.2. Reverse Shock Emission from Pair-Rich or Neutron-Fed GRB Ejecta.* Beside magnetic fields, other components of the GRB ejecta, if present, could also alter the reverse shock emission features, such as $e^\pm$ pairs and neutrons [26, 88].

The intrinsic GRB spectrum may extend to very high energy, so that the optical depth to $\gamma$-$\gamma$ absorption for the most energetic photons at the high energy end of the spectrum may exceed unity. In this case, intense pair production may occur in the prompt emission phase and $e^\pm$ pairs remain in the fireball, with the same bulk Lorentz factor as the fireball (static in the comoving frame). Since the $e^\pm$ pair will also share energy in the reverse shock, the reverse shock emission spectrum is altered, and the peak is softened to lower frequencies. It turns out that a pair-rich reverse shock gives rise to stronger radiation in the IR band, instead of the optical/UV emission in the case where pair-loading is negligible [26]. The optical afterglow signal may suffer significant dust obscuration since long GRBs are usually expected to occur within star forming regions; observable IR flashes could test this issue, provided that IR detector can be slewed rapidly enough to respond the GRB trigger [26].

It has also been pointed out that GRB ejecta may contain a significant fraction of neutrons [88, 141–143], which would cause much more complex dynamics for the system than in the neutron-free case. In general, the neutron shells ($N$-ejecta) would freely penetrate through the charged ion shells ($I$-ejecta) in front of them and would separate from the $I$-ejecta more and more, while the $I$-ejecta suffer deceleration from internal shocks. The $N$-ejecta would decelerate by collecting ambient medium and the mass of fast neutrons would decrease as the result of $\beta$-decay. The neutron decay products and the shocked medium will form new ejecta ($T$-ejecta) that follow behind the $N$-ejecta and the interactions between these three ejecta would give rise to rich radiation features. For an ISM type medium, the $T$-ejecta move faster than the $I$-ejecta, so that the $T$-ejecta would first interact with the $N$-ejecta or ambient medium, but the reverse shock emission in this stage would be out-shined by the forward shock emission. Later on, the $I$-ejecta would catch up the $T$-ejecta and a prominent bump signature around tens to hundreds of seconds would show up, which is mainly

dominated by the refreshed reverse shock emission. For a stellar wind type medium, $I$-ejecta would pick up the $T$-ejecta first and then collide with the $N$-ejecta and ambient medium. In this case, three components contribute to the final emission, that is, the forward shock emission, the reverse shock emission from the shocked $I$-ejecta, and the shocked $T$-ejecta emission. A typical neutron-rich wind-interaction lightcurve is characterized by a prominent early plateau lasting for ~100 s, followed by normal power-law decay [88].

*3.3. High Energy Photons and Neutrinos from Reverse Shock.* Since the number of heated electrons in region 3 is $\eta$ ($10^2$–$10^3$) times higher than in region 2, a strong synchrotron self-Compton (SSC) emission in region 3 is expected, especially when reverse shock emission is prominent [9, 89, 90, 144]. The SSC emission feature is essentially determined by the random Lorentz factors of the electrons $\gamma_e$, since the seed photons mainly are concentrated in the optical band. When $\gamma_e$ is of the order of 1000 or even higher, the SSC emission from the reverse shock could dominate over the synchrotron and other IC emissions in the energy bands from tens of MeV to tens of GeV, while the cross-IC (and/or the forward shock SSC emissions) becomes increasingly dominant at TeV energy bands [89, 90]. When $\gamma_e$ is of order 100, if the SSC process dominates the cooling of shocked electrons, the majority of the shock energy would be radiated in the second-order scattering at 10–100 MeV, and the first-order scattering may give rise to X-ray flares in the very early afterglow phase [144]. In this case, the optical flash (due to synchrotron) is highly suppressed.

On the other hand, it has been proposed that when GRBs erupt in a stellar wind, usually the region 2 and region 3 still have overlap with the prompt MeV $\gamma$-ray emission site at the reverse shock crossing phase [80, 145]. Such overlapping could lead to significant modifications of the early afterglow emission, since the dominant cooling process for the electrons is likely to be the IC process with the MeV photons [145]. Due to the close overlap of the MeV photon flow and the shocked regions, the newly upscattered high energy photons would be absorbed by the MeV photons to generate $e^{\pm}$ pairs and then rescatter the soft X-rays to power a detectable sub-GeV signal [80]. Other than that, $10^{14}$ eV neutrino emission is also expected from interactions between shocked protons and the MeV photon flow [80]. Alternatively, high energy neutrinos are also expected from reverse shocks as the GRB jets crossing the stellar envelop, either for choked or for successful relativistic jets [146].

*3.4. Long Lasting Reverse Shocks.* In the standard model, a uniform distribution of the bulk Lorentz factors in the GRB ejecta is assumed. However, in principle GRB ejecta could have a range of bulk Lorentz factors, so that the inner (lower $\gamma$) parts may carry most of the mass or even most of the energy, for example, $\gamma Mc^2 \propto \gamma^{-s+1}$ [83, 147, 148]. In this case, the low Lorentz factor part of the ejecta will catch up with the high Lorentz factor part when the latter is decelerated by the ambient medium; thus, a long-lasting weak reverse shock could develop, until the whole ejecta have been shocked. Analogously to the standard model, this process could also be classified analytically into two cases: the thick shell case and the thin shell case [83], and it turns out that, in the thick shell case, the reverse shock is strong and may give rise to the plateau observed in the early optical and X-ray afterglows [83]. Considering more complicated stratification profiles for the ejecta properties (e.g., Lorentz factor, luminosity, and density), the long lasting reverse shock emission could be endowed with a richer set of features, including reproducing the canonical X-ray lightcurve as observed by *Swift*, as long as the forward shock emission can somehow be suppressed [84, 85].

*3.5. Polarization of Reverse Shock Emission.* If the GRB ejecta contain large scale ordered magnetic fields, the prompt $\gamma$-ray emission and the reverse shock emission should be polarized [149]. However, aside from any instrumental difficulties, making unequivocal polarization determinations that prove this is still challenging [149, 150]. Furthermore, a high degree of linear polarization in the prompt $\gamma$-rays is also possible in the presence of a random magnetic field, arguably originating in electromagnetic instabilities that develop at the collisionless shock [151]. In any case, polarization measurements of the reverse shock emission could place strong constraints on the strength and perhaps also the structure of the magnetic field within the GRB outflow. The RINGO detector on the Liverpool Telescope has reported an optical polarization of GRB 090102 ($P = 101\%$) [152] and GRB 060418 ($P < 8\%$) [153], but a larger sample is definitely needed to give general discussion on the properties of GRB outflow [150].

## 4. Connection between Theory and Observations of the Reverse Shock Emission

*4.1. Theory Predictions of Observational Features of Reverse Shocks.* According to the standard external shock theory, reverse shocks would mainly contribute to the early optical afterglow (if not suppressed) [13]. For the ISM model, the early optical lightcurve of the reverse shock would increase proportional to $t^5$ (thin shell case) or $t^{1/2}$ (thick shell case) and then decrease with a general slope $\sim t^{-2}$ [54, 58]. For the wind model, the lightcurve would increase initially with slope $t^{5/2}$ when synchrotron self-absorption becomes important in this case and then rise with slope 1/2 for both thin and thick cases to finally decrease with a slope $\sim t^{-3}$, determined by the angular time delay effect [70].

The morphology of early optical afterglows essentially depends on the relative relation between the forward shock and reverse shock emission. In general, the early optical afterglows for constant density medium model were usually classified into three types (see Figure 2):

(i) Type I: rebrightening. Two peaks emerge in this type of lightcurve. The first peak is dominated by the reverse shock emission, and the rebrightening signature comes from the forward shock emission. The temporal index for the rebrightening depends on

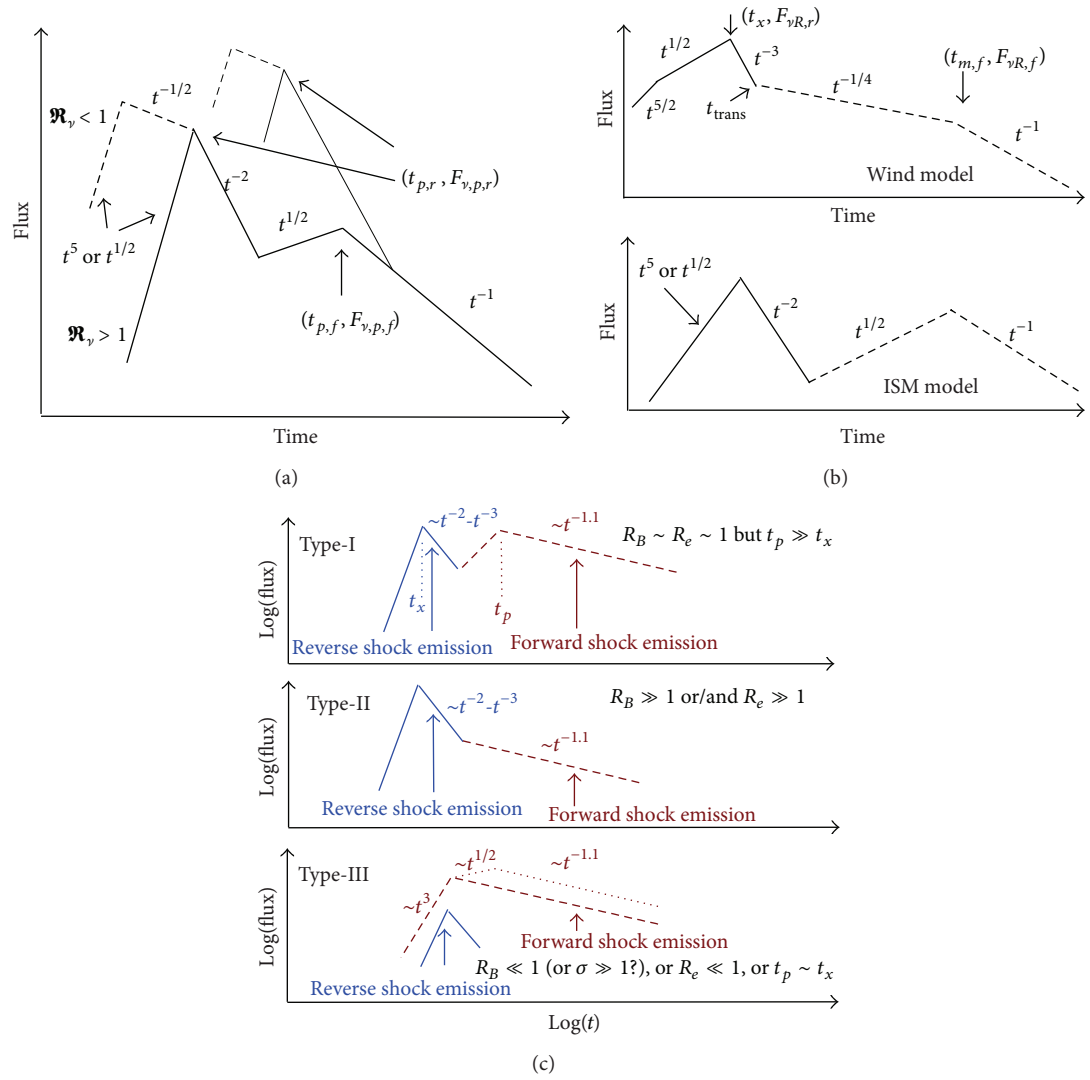


FIGURE 2: Theoretically expected early optical afterglow lightcurves from reverse plus forward shock emission and illustrative diagram of three classified types: (a) from [58]; (b) from [70]; (c) from [92].

the specific forward shock model and the spectral regimes, which are collected in [13].

(ii) Type II: flattening. In this case, the forward shock emission peak is under the reverse shock component, and the decaying part of the forward shock emission shows up later when the reverse shock component is getting fainter more rapidly.

(iii) Type III: no reverse shock component. Two reasons may be responsible for this, one being that the reverse shock component is weak compared with the forward shock emission and the other being that the reverse shock component is completely suppressed for some reason as proposed by some extended models (see Section 3), such as magnetic fields dominating the ejecta [73], $e^{\pm}$ pair effects [26], or SSC process in the reverse shock region [89, 90, 144].

Recently, it is suggested that an insight into the $\nu_m^f(T_x)$ value could lead to strong constraints on relevant afterglow parameters [91], so that the forward shock dominated cases (Type III) should be redefined into two categories:

Type III: forward shock dominated lightcurves without $\nu_m$ crossing;

Type IV: forward shock dominated lightcurves with $\nu_m$ crossing.

*4.2. Identification of Reverse Shock Emission from Observational Data.* Based on the theoretically predicted features, once prompt optical observations are obtained, the reverse shock components could be identified with the following procedure:

(1) Compare the first optical observation time $t_s$ and the $\gamma$-ray duration $T_{90}$. If $t_s < T_{90}$, check the variability level of the optical signal. For cases with significant

variability, ascertain the relation between optical variability and $\gamma$-ray variability with correlation cross checking method. Bursts with $t_s > T_{90}$ or $t_s < T_{90}$ but with weak variability (or with significant variability but no correlation with $\gamma$-ray signal) may be taken as candidates for having a reverse shock signal. It is worth pointing out that variability within a certain level may be explained within the external shock framework, such as invoking density fluctuation, inhomogeneous jets, or neutron decay signatures [88, 154–156]. Information from other observational bands (radio, X-ray, and high energy $\gamma$-rays) would be helpful to make a stricter selection between cases.

(2) Fit the optical lightcurve with a multisegment broken power law function. If the initial decay slope of the signal is close to $t^{-2}$ (ISM) or $t^{-3}$ (wind), check whether the following decay or rising slopes are consistent with the forward shock predictions [13] and classify the candidate bursts as one of the four types defined above.

(3) Plot the multiband spectrum of the early afterglow, if possible, and verify if there is evidence for the existence of two components, for example, forward shock component (usually peaks at X-ray) and reverse shock component (usually peaks at optical).

*4.3. Constraints on Theoretical Parameters from Observational Results.* Valuable results may be expected in the case of bursts where multiband (instead of only X-ray) early afterglow observations are available, especially for the properties of the GRB outflow itself. For cases with identifiable reverse shock component, several important pieces of information, if available, should be useful to constrain model parameters:

(i) Consider the rising and decaying slope of the reverse shock peak. The decaying slope is always in handy since it is the key parameter to identify the reverse shock component. It could be used to differentiate the CBM profile, for example, $t^{-2}$ for ISM and $t^{-3}$ for wind. On the other hand, it is also useful to constrain the electron energy distribution index, $p_r$, where the subscript $r$ ($f$) denotes reverse (forward) shock, although the constraint is weak; otherwise, the decay slope would not be general enough for verifying the reverse shock emission. The rising slope of the reverse shock is usually missing from the current data, due to the limited capability of existing facilities (e.g., slewing speed of the dedicated telescopes) and the short-lived nature of the lightcurve rise phase. However, once the rising slope becomes available, not only it is useful for obtaining the CBM profile, but also it is helpful for testing some proposed extended models, such as the neutron-fed outflow model (see details in Section 3).

(ii) The reverse shock peaking time is usually related to the shock crossing time $T_x$, which is useful to determine the initial physical conditions within the GRB ejecta, specifically its Lorentz factor $\eta$ and width $\Delta$. But one needs to keep in mind that the first available observational time may not represent the reverse shock peaking time, especially when the rising part of the lightcurve is missing. For those cases, only upper limits could be made for $T_x$.

(iii) Based on the standard synchrotron external shock model and assigning reasonable ranges of a set of model parameters, one can constrain relevant parameters by fitting the overall observational lightcurve and the broadband spectrum, if available. However, in this approach, too many unknown free parameters are involved, for example, the density of CBM, the isotropic equivalent kinetic energy of the ejecta, the initial Lorentz factor of the ejecta, and especially the microphysics parameters in the shock region ($\epsilon_{e,r}$, $\epsilon_{e,f}$, $\epsilon_{B,r}$, $\epsilon_{e,f}$, $p_r$, and $p_f$). Since the observational information is usually not adequate to constrain so many parameters, some *ad hoc* assumptions are commonly used; for instance, the values of the microphysical parameters in the forward and reverse shock region are assumed the same. It is worth pointing out that the relation between $\epsilon_{B,r}$ and $\epsilon_{B,f}$ should be treated carefully, since it is useful for diagnosing the magnetization degree of the initial outflow.

(iv) Beside fitting the overall lightcurves, some important parameters such as the Lorentz factor and the magnetization degree of the initial outflow could also be constrained by working on the "ratios" of the quantities for both shocks, especially at $T_x$ [58, 70]:

$$\frac{\nu_{m,r}(T_x)}{\nu_{m,f}(T_x)} \sim \widehat{\gamma}^{-2}\mathcal{R}_B,$$
$$\frac{\nu_{c,r}(T_x)}{\nu_{c,f}(T_x)} \sim \mathcal{R}_B^{-3}, \tag{27}$$
$$\frac{F_{\nu,m,r}(T_x)}{F_{\nu,m,f}(T_x)} \sim \widehat{\gamma}\mathcal{R}_B,$$

where $\nu_m$, $\nu_c$, and $F_{\nu,m}$ are the typical frequency, cooling frequency, and the peak flux for synchrotron spectrum, and

$$\widehat{\gamma} \equiv \frac{\gamma_\times^2}{\eta} = \min\left(\eta, \frac{\gamma_c^2}{\eta}\right),$$
$$\mathcal{R}_B \equiv \left(\frac{\epsilon_{B,r}}{\epsilon_{B,f}}\right)^{1/2}, \tag{28}$$

where $\gamma_c$ is a critical initial Lorentz factor which divides the thin shell and thick shell regimes [58]. This paradigm provides a straightforward recipe for directly constraining $\eta$ and $\mathcal{R}_B$ (essentially the magnetization degree of the initial outflow) using early optical afterglow data only. Moreover, the absolute values of the poorly known model parameters related to the shock microphysics (e.g., $\epsilon_e$, $p$) do not enter the problem, since they largely cancel out once they are assumed to have the same value in both shocks.

Table 1: GRBs with claimed reverse shock signatures and the corresponding references.

| Name | References |
|---|---|
| GRB 990123 | [22, 52, 55, 56, 61, 63, 94–105] |
| GRB 021004 | [25, 106] |
| GRB 021211 | [49, 60, 61, 107, 108] |
| GRB 050525A | [109, 110] |
| GRB 050904 | [111–114] |
| GRB 060111B | [105, 115] |
| GRB 060117 | [116] |
| GRB 060908 | [117] |
| GRB 061126 | [118, 119] |
| GRB 080319B | [120–123] |
| GRB 081007 | [124] |
| GRB 090102 | [125, 126] |
| GRB 090424 | [124] |
| GRB 090902B | [127, 128] |
| GRB 091024 | [129] |
| GRB 110205A | [130–132] |
| GRB 130427A | [133–136] |

(v) A morphological analysis of the early optical lightcurves can also provide direct model constraints. Given a sample of optical lightcurves with early detections, one can divide them into different categories based on their shapes, then calculate the ratio between each category, and find out the right parameter regimes that can reproduce these ratios with Monte Carlo simulations [91].

(vi) As mentioned above, time variability within certain modest limits in the lightcurve might contain information on some interesting properties, such as external density fluctuations, inhomogeneous jets, or neutron decay signatures.

## 5. Current Observational Results on Reverse Shock Emission

It has been 15 years since the first prompt optical flash was discovered and was interpreted with a reverse shock model (e.g., GRB 990123 [22, 51, 52]). We have searched the literature since then, finding that 17 GRBs have been claimed to have reverse shock signature (3 in the pre-*Swift* era). The detection rate is much lower than expected. Each of these bursts has been interpreted in great detail. In Table 1, we collect the burst identifiers and their relevant references to the individual studies on those bursts.

Most recently, a comprehensive statistical analysis of reverse shock emission in the optical afterglows of GRBs was carried out [157]. Here we briefly summarize the results as follows:

(i) With stricter criteria, such as requiring redshift measurement, a full sample of 10 GRBs with reverse shock signatures was identified: GRBs 990123, 021004, 021211, 060908, 061126, 080319B, 081007, 090102, 090424, and 130427A. For five of them, a reverse shock component has been firmly confirmed (e.g., GRB 990123 [51], GRB 021211 [25, 59], GRB 061126 [118], GRB 081007 [124], and GRB 130427A [133, 158]). For the remaining five cases, different interpretations (other than the reverse shock emission) can be applicable for the early observational results, due to the lack of good early-time photometric coverage.

(ii) In the sample, GRB 012004 is the only case with a possible Type I lightcurve (in which both reverse and forward shock afterglow lightcurve peaks are observed) and the other nine cases are all with Type II lightcurves (in which the characteristic steep-to-shallow lightcurve evolution is observed).

(iii) Based on the analytic reverse shock plus forward shock model, the physical quantities describing the ejecta and CBM are explored by reproducing the observed optical lightcurves of the sample with Monte Carlo simulations, with the result that the physical properties cover a wide parameter space and do not seem to cluster around any preferential values, which is consistent with previous analyses that concentrated on late time forward shock emission [19, 20].

(iv) It is suggested that GRBs with an identifiable reverse shock component show high magnetization parameter $\mathcal{R}_B \sim \sqrt{2}$–$10^2$. Together with the fact that 9/10 of the cases in the sample belong to Type II, the results are in agreement with the mildly magnetized baryonic jet model of GRBs [73].

## 6. Summary and Prospects for Reverse Shock Studies

Reverse shock emission is a natural prediction of the standard external shock GRB afterglow model, and it has been firmly confirmed in a small number of cases. Since the reverse shock emission is directly related to the GRB outflow itself, investigating the nature of reverse shock emission would lead to a better understanding of the intrinsic properties of the GRB ejecta, which is essential for constructing a complete picture of the GRB physics.

A theoretical framework for the behavior of the reverse shock emission under various conditions was developed, mostly before the launch of *Swift* (and even before the first relevant discovery of GRB 990123), and expected features were discussed for inferring various intrinsic properties of the GRB ejecta. *Swift* was launched, in part, with hopes to make significant progress on this specific problem. After a decade of highly successful operation, *Swift* indeed has collected a good sample of early afterglow lightcurves to allow detailed studies of GRB reverse shocks. While the size of the sample is still limited, nonetheless, it appears that the number of bursts with confirmed reverse shock components is much lower than the expectation from the standard model.

The mismatch between this theoretical expectation and the observations could be intrinsic or it could be systematically biased due to the limitations of current ground-based observational facilities. If it is intrinsic, the origin of the suppression of the reverse shock emission for most of GRBs would shed new light on the composition problem of GRB jets; for example, most of the jets might be highly magnetized.

Based on current observational results, more reliable results could also be achieved by including more broadband or more specialized information instead of just photometric or spectroscopic optical data. For instance, one could use early radio data or (sub)mm data [159, 160] to search for reverse shock emission signatures [133, 161]; one could identify the reverse shock components and diagnose the structure of the magnetic fields in GRB ejecta via the detection of early time optical polarization [152, 153]; one could estimate the magnetization degree of the GRB jets by comprehensive considering of the $\gamma$-ray spectrum [162], the early optical lightcurve type, and special X-ray afterglow features, such as the X-ray plateau due to late magnetic energy injection [73].

At this point, the main problem is that there is still a large fraction of GRBs lacking early optical observations, and a more complete sample is required for firmer conclusions. Some upcoming facilities may help with this issue, such as the Chinese-French mission SVOM [163] and especially its key element, the Ground Wide Angle Cameras (GWACs). The GWACs are an array of wide field of view (about 8000 $\deg^2$, with a sensitivity of about 15 magnitudes at 5 s) optical cameras operating in the optical domain. It will monitor continuously the field covered by the SVOM $\gamma$-ray detector ECLAIRs, in order to observe the visible emission of more than 20% of the events, at least 5 minutes before and 15 minutes after the GRB trigger. This and other ground-based facilities may key in making further progress in this field.

## Conflict of Interests

The authors declare that there is no conflict of interests regarding the publication of this paper.

## Acknowledgment

This work was supported in part by NASA NNX 13AH50G.

## References

[1] B. Zhang and P. Mészáros, "Gamma-ray bursts: progress, problems & prospects," *International Journal of Modern Physics A*, vol. 19, no. 15, pp. 2385–2472, 2004.

[2] T. Piran, "Gamma-ray bursts and the fireball model," *Physics Report*, vol. 314, no. 6, pp. 575–667, 1999.

[3] P. Mészros, "Gamma-ray bursts," *Reports on Progress in Physics*, vol. 69, pp. 2259–2322, 2006.

[4] B. Zhang, "Gamma-ray bursts in the swift era," *Chinese Journal of Astronomy and Astrophysics*, vol. 7, no. 1, 2007.

[5] P. Kumar and B. Zhang, "The physics of gamma-ray bursts and relativistic jets," *Physics Reports*, vol. 561, pp. 1–109, 2015.

[6] B. Zhang, "Gamma-ray burst prompt emission," *International Journal of Modern Physics D*, vol. 23, no. 2, Article ID 1430002, 2014.

[7] M. J. Rees and P. Meszaros, "Relativistic fireballs: energy conversion and time-scales," *Monthly Notices of the Royal Astronomical Society*, vol. 258, no. 1, pp. 41P–43P, 1992.

[8] M. J. Rees and P. Mészáros, "Unsteady outflow models for cosmological gamma-ray bursts," *The Astrophysical Journal*, vol. 430, no. 2, pp. L93–L96, 1994.

[9] P. Mészáros and M. J. Rees, "Relativistic fireballs and their impact on external matter: models for cosmological gamma-ray bursts," *Astrophysical Journal Letters*, vol. 405, no. 1, pp. 278–284, 1993.

[10] P. Mészáros and M. J. Rees, "Optical and long-wavelength afterglow from gamma-ray bursts," *Astrophysical Journal Letters*, vol. 476, no. 1, pp. 232–237, 1997.

[11] R. Sari, T. Piran, and R. Narayan, "Spectra and light curves of gamma-ray burst afterglows," *The Astrophysical Journal Letters*, vol. 497, no. 1, pp. L17–L20, 1998.

[12] R. A. Chevalier and Z.-Y. Li, "Wind interaction models for gamma-ray burst afterglows: the case for two types of progenitors," *Astrophysical Journal Letters*, vol. 536, no. 1, pp. 195–212, 2000.

[13] H. Gao, W.-H. Lei, Y.-C. Zou, X.-F. Wu, and B. Zhang, "A complete reference of the analytical synchrotron external shock models of gamma-ray bursts," *New Astronomy Reviews*, vol. 57, no. 6, pp. 141–190, 2013.

[14] R. A. M. J. Wijers, M. J. Rees, and P. Mészáros, "Shocked by GRB 970228: the afterglow of a cosmological fireball," *Monthly Notices of the Royal Astronomical Society*, vol. 288, no. 4, pp. L51–L56, 1997.

[15] E. Waxman, "Gamma-ray-burst afterglow: supporting the cosmological fireball model, constraining parameters, and making predictions," *Astrophysical Journal Letters*, vol. 485, no. 1, pp. L5–L8, 1997.

[16] R. A. M. J. Wijers and T. J. Galama, "Physical parameters of GRB 970508 and GRB 971214 from their afterglow synchrotron emission," *The Astrophysical Journal*, vol. 523, no. 1, pp. 177–186, 1999.

[17] Y. F. Huang, Z. G. Dai, and T. Lu, "A generic dynamical model of gamma-ray burst remnants," *Monthly Notices of the Royal Astronomical Society*, vol. 309, no. 2, pp. 513–516, 1999.

[18] Y. F. Huang, L. J. Gou, Z. G. Dai, and T. Lu, "Overall evolution of jetted gamma-ray burst ejecta," *The Astrophysical Journal*, vol. 543, no. 1, pp. 90–96, 2000.

[19] A. Panaitescu and P. Kumar, "Fundamental physical parameters of collimated gamma-ray burst afterglows," *Astrophysical Journal Letters*, vol. 560, no. 1, pp. L49–L53, 2001.

[20] A. Panaitescu and P. Kumar, "Properties of relativistic jets in gamma-ray burst afterglows," *Astrophysical Journal Letters*, vol. 571, no. 2, pp. 779–789, 2002.

[21] S. A. Yost, F. A. Harrison, R. Sari, and D. A. Frail, "A study of the afterglows of four gamma-ray bursts: constraining the explosion and fireball model," *Astrophysical Journal Letters*, vol. 597, no. 1, pp. 459–473, 2003.

[22] C. Akerlof, R. Balsano, S. Barthelmy et al., "Observation of contemporaneous optical radiation from a $\gamma$-ray burst," *Nature*, vol. 398, no. 6726, pp. 400–402, 1999.

[23] F. A. Harrison, J. S. Bloom, D. A. Frail et al., "Optical and radio observations of the afterglow from GRB 990510: evidence for a jet," *Astrophysical Journal Letters*, vol. 523, no. 2, pp. L121–L124, 1999.

[24] E. Berger, S. R. Kulkarni, G. Pooley et al., "A common origin for cosmic explosions inferred from calorimetry of GRB030329," *Nature*, vol. 426, no. 6963, pp. 154–157, 2003.

[25] D. W. Fox, S. Yost, S. R. Kulkarni et al., "Early optical emission from the $\gamma$-ray burst of 4 October 2002," *Nature*, vol. 422, no. 6929, pp. 284–286, 2003.

[26] W. Li, A. V. Filippenko, R. Chornock, and S. Jha, "The early light curve of the optical afterglow of GRB 021211," *Astrophysical Journal Letters*, vol. 586, no. 1, pp. L9–L12, 2003.

[27] N. Gehrels, G. Chincarini, P. Giommi et al., "The swift gamma-ray burst mission," *Astrophysical Journal Letters*, vol. 611, no. 2, pp. 1005–1020, 2004.

[28] G. Tagliaferri, M. Goad, G. Chincarini et al., "An unexpectedly rapid decline in the X-ray afterglow emission of long $\gamma$-ray bursts," *Nature*, vol. 436, no. 7053, pp. 985–988, 2005.

[29] D. N. Burrows, P. Romano, A. Falcone et al., "Astrophysics: bright X-ray flares in gamma-ray burst afterglows," *Science*, vol. 309, no. 5742, pp. 1833–1835, 2005.

[30] B. Zhang, Y. Z. Fan, J. Dyks et al., "Physical processes shaping gamma-ray burst X-ray afterglow light curves: theoretical implications from the swift X-ray telescope observations," *The Astrophysical Journal*, vol. 642, no. 1, pp. 354–370, 2006.

[31] J. A. Nousek, C. Kouveliotou, D. Grupe et al., "Evidence for a canonical gamma-ray burst afterglow light curve in the swift XRT data," *The Astrophysical Journal*, vol. 642, no. 1, pp. 389–400, 2006.

[32] P. T. O'Brien, R. Willingale, J. Osborne et al., "The early X-ray emission from GRBs," *Astrophysical Journal Letters*, vol. 647, no. 2, pp. 1213–1237, 2006.

[33] P. A. Evans, A. P. Beardmore, K. L. Page et al., "Methods and results of an automatic analysis of a complete sample of Swift-XRT observations of GRBs," *Monthly Notices of the Royal Astronomical Society*, vol. 397, no. 3, pp. 1177–1201, 2009.

[34] D. N. Burrows, J. E. Hill, J. A. Nousek et al., "The wift X-ray telescope," *Space Science Reviews*, vol. 120, no. 3-4, pp. 165–195, 2005.

[35] Y. Z. Fan and D. M. Wei, "Late internal-shock model for bright X-ray flares in gamma-ray burst afterglows and GRB 011121," *Monthly Notices of the Royal Astronomical Society: Letters*, vol. 364, no. 1, pp. L42–L46, 2005.

[36] B.-B. Zhang, E. N.-W. Liang, and B. Zhang, "A comprehensive analysis of Swift XRT data. I. Apparent spectral evolution of gamma-ray burst X-ray tails," *Astrophysical Journal*, vol. 666, no. 2 I, pp. 1002–1011, 2007.

[37] E. N.-W. Liang and B.-B. Zhang, "A comprehensive analysis of Swift XRT data. II. Diverse physical origins of the shallow decay segment," *The Astrophysical Journal*, vol. 670, no. 1, pp. 565–583, 2007.

[38] E.-W. Liang, J. L. Racusin, B. Zhang, B.-B. Zhang, and D. N. Burrows, "A comprehensive analysis of Swift XRT data. III. Jet break candidates in X-ray and optical afterglow light curves," *Astrophysical Journal*, vol. 675, no. 1, pp. 528–552, 2008.

[39] E.-W. Liang, H.-J. Lü, S.-J. Hou, B.-B. Zhang, and B. Zhang, "A comprehensive analysis of swift/X-ray telescope data. IV. single power-law decaying light curves versus canonical light curves and implications for a unified origin of X-rays," *Astrophysical Journal Letters*, vol. 707, no. 1, pp. 328–342, 2009.

[40] N. R. Butler and D. Kocevski, "X-ray hardness evolution in GRB afterglows and flares: late-time GRB activity without NH variations," *Astrophysical Journal*, vol. 663, pp. 407–419, 2007.

[41] D. Kocevski, N. Butler, and J. S. Bloom, "Pulse width evolution of late-time X-ray flares in gamma-ray bursts," *Astrophysical Journal*, vol. 667, no. 2 I, pp. 1024–1032, 2007.

[42] G. Chincarini, A. Moretti, P. Romano et al., "The first survey of X-ray flares from gamma-ray bursts observed by Swift: temporal properties and morphology," *Astrophysical Journal*, vol. 671, no. 2, pp. 1903–1920, 2007.

[43] G. Chincarini, J. Mao, R. Margutti et al., "Unveiling the origin of X-ray flares in gamma-ray bursts," *Monthly Notices of the Royal Astronomical Society*, vol. 406, no. 4, pp. 2113–2148, 2010.

[44] R. Margutti, C. Guidorzi, G. Chincarini et al., "Lag-luminosity relation in $\gamma$-ray burst X-ray flares: a direct link to the prompt emission," *Monthly Notices of the Royal Astronomical Society*, vol. 406, no. 4, pp. 2149–2167, 2010.

[45] B. Zhang, "Open questions in GRB physics," *Comptes Rendus Physique*, vol. 12, no. 3, pp. 206–225, 2011.

[46] Y. C. Zou, F. Y. Wang, and K. S. Cheng, "Long-term X-ray emission from Swift J1644+57," *Monthly Notices of the Royal Astronomical Society*, vol. 434, no. 4, pp. 3463–3468, 2013.

[47] R. Sari and T. Piran, "Hydrodynamic timescales and temporal structure of gamma-ray bursts," *Astrophysical Journal Letters*, vol. 455, no. 2, pp. L143–L146, 1995.

[48] R. Sari and T. Piran, "Predictions for the very early afterglow and the optical flash," *The Astrophysical Journal*, vol. 520, no. 2, pp. 641–649, 1999.

[49] D. W. Fox, P. A. Price, A. M. Soderberg et al., "Discovery of early optical emission from GRB 021211," *Astrophysical Journal Letters*, vol. 586, no. 1, pp. L5–L8, 2003.

[50] D. A. Frail, S. R. Kulkarni, E. Berger, and M. H. Wieringa, "A complete catalog of radio afterglows: the first five years," *Astronomical Journal*, vol. 125, no. 5, pp. 2299–2306, 2003.

[51] R. Sari and T. Piran, "GRB 990123: the optical flash and the fireball model," *The Astrophysical Journal*, vol. 517, no. 2, pp. L109–L112, 1999.

[52] P. Mészáros and M. J. Rees, "GRB 990123: reverse and internal shock flashes and late afterglow behaviour," *Monthly Notices of the Royal Astronomical Society*, vol. 306, no. 3, pp. L39–L43, 1999.

[53] S. Kobayashi and R. Sari, "Optical flashes and radio flares in gamma-ray burst afterglow: numerical study," *The Astrophysical Journal*, vol. 542, no. 2, pp. 819–828, 2000.

[54] S. Kobayashi, "Light curves of gamma-ray burst optical flashes," *Astrophysical Journal Letters*, vol. 545, no. 2, pp. 807–812, 2000.

[55] X. Y. Wang, Z. G. Dai, and T. Lu, "Intrinsic parameters of GRB 990123 from its prompt optical flash and afterglow," *Monthly Notices of the Royal Astronomical Society*, vol. 319, no. 4, pp. 1159–1162, 2000.

[56] Y. Z. Fan, Z. G. Dai, Y. F. Huang et al., "Optical flash of GRB 990123: constraints on the physical parameters of the reverse shock," *Chinese Journal of Astronomy and Astrophysics*, vol. 2, no. 5, pp. 449–453, 2002.

[57] S. Kobayashi and B. Zhang, "GRB 021004: reverse shock emission," *The Astrophysical Journal Letters*, vol. 582, no. 2, pp. L75–L78, 2003.

[58] B. Zhang, S. Kobayashi, and P. Mészáros, "Gamma-ray burst early optical afterglows: implications for the initial lorentz factor and the central engine," *Astrophysical Journal Letters*, vol. 595, no. 2 I, pp. 950–954, 2003.

[59] D. M. Wei, "The afterglow of GRB 021211: another case of reverse shock emission," *Astronomy and Astrophysics*, vol. 402, pp. L9–L12, 2003.

[60] P. Kumar and A. Panaitescu, "A unified treatment of the gamma-ray burst 021211 and its afterglow," *Monthly Notices of the Royal Astronomical Society*, vol. 346, no. 3, pp. 905–914, 2003.

[61] A. Panaitescu and P. Kumar, "Analysis of two scenarios for the early optical emission of the gamma-ray burst afterglows 990123 and 021211," *Monthly Notices of the Royal Astronomical Society*, vol. 353, no. 2, pp. 511–522, 2004.

[62] E. Nakar and T. Piran, "Early afterglow emission from a reverse shock as a diagnostic tool for gamma-ray burst outflows," *Monthly Notices of the Royal Astronomical Society*, vol. 353, no. 2, pp. 647–653, 2004.

[63] A. M. Soderberg and E. Ramirez-Ruiz, "Flaring up: radio diagnostics of the kinematic, hydrodynamic and environmental properties of gamma-ray bursts," *Monthly Notices of the Royal Astronomical Society*, vol. 345, no. 3, pp. 854–864, 2003.

[64] E. S. Rykoff, D. A. Smith, P. A. Price et al., "The early optical afterglow of GRB 030418 and progenitor mass loss," *The Astrophysical Journal Letters*, vol. 601, no. 2, pp. 1013–1018, 2004.

[65] G. G. Williams, H. S. Park, and R. Porrata, "GRB 991106, LOTIS optical observations," *GRB Coordinates Network*, vol. 437, p. 1, 1999.

[66] A. Klotz and J. L. Atteia, "GRB 030324: TAROT optical observations," *GRB Coordinates Network*, vol. 1961, p. 1, 2003.

[67] K. Torii, "GRB 030528: optical observations at RIKEN," Tech. Rep. 2253:1, GRB Coordinates Network, 2003.

[68] K. Torii, "GRB 030913: optical limit at RIKEN," *GRB Coordinates Network*, vol. 2381, p. 1, 2003.

[69] X. F. Wu, Z. G. Dai, Y. F. Huang, and T. Lu, "Optical flashes and very early afterglows in wind environments," *Monthly Notices of the Royal Astronomical Society*, vol. 342, no. 4, pp. 1131–1138, 2003.

[70] S. Kobayashi and B. Zhang, "Early optical afterglows from wind-type gamma-ray bursts," *Astrophysical Journal Letters*, vol. 597, no. 1, pp. 455–458, 2003.

[71] Y. C. Zou, X. F. Wu, and Z. G. Dai, "Early afterglows in wind environments revisited," *Monthly Notices of the Royal Astronomical Society*, vol. 363, no. 1, pp. 93–106, 2005.

[72] S.-X. Yi, X.-F. Wu, and Z.-G. Dai, "Early afterglows of gamma-ray bursts in a stratified medium with a power-law density distribution," *The Astrophysical Journal*, vol. 776, no. 2, article 120, 2013.

[73] B. Zhang and S. Kobayashi, "Gamma-ray burst early afterglows: reverse shock emission from an arbitrarily magnetized ejecta," *Astrophysical Journal Letters*, vol. 628, no. 1 I, pp. 315–334, 2005.

[74] Y. Z. Fan, D. M. Wei, and C. F. Wang, "The very early afterglow powered by ultra-relativistic mildly magnetized outflows," *Astronomy & Astrophysics*, vol. 424, no. 2, pp. 477–484, 2004.

[75] P. Mimica, D. Giannios, and M. A. Aloy, "Deceleration of arbitrarily magnetized GRB ejecta: the complete evolution," *Astronomy and Astrophysics*, vol. 494, no. 3, pp. 879–890, 2009.

[76] P. Mimica, D. Giannios, and M. A. Aloy, "Multiwavelength afterglow light curves from magnetized gamma-ray burst flows," *Monthly Notices of the Royal Astronomical Society*, vol. 407, no. 4, pp. 2501–2510, 2010.

[77] Y. Mizuno, B. Zhang, B. Giacomazzo et al., "Magnetohydrodynamic effects in propagating relativistic jets: reverse shock and magnetic acceleration," *The Astrophysical Journal Letters*, vol. 690, no. 1, pp. L47–L51, 2009.

[78] R. Harrison and S. Kobayashi, "Magnetization degree of gamma-ray burst fireballs: numerical study," *Astrophysical Journal*, vol. 772, no. 2, article 101, 2013.

[79] Z. Li, Z. G. Dai, T. Lu, and L. M. Song, "Pair loading in gamma-ray burst fireballs and prompt emission from pair-rich reverse shocks," *The Astrophysical Journal*, vol. 599, no. 1 I, pp. 380–386, 2003.

[80] Y. Z. Fan, B. Zhang, and D. M. Wei, "Early photon-shock interaction in a stellar wind: a sub-GeV photon flash and high-energy neutrino emission from long gamma-ray bursts," *The Astrophysical Journal*, vol. 629, no. 1, pp. 334–340, 2005.

[81] F. Genet, F. Daigne, and R. Mochkovitch, "Can the early X-ray afterglow of gamma-ray bursts be explained by a contribution from the reverse shock?" *Monthly Notices of the Royal Astronomical Society*, vol. 381, no. 2, pp. 732–740, 2007.

[82] Z. L. Uhm and A. M. Beloborodov, "On the mechanism of gamma-ray burst afterglows," *The Astrophysical Journal*, vol. 665, no. 2, pp. L93–L96, 2007.

[83] X.-W. Liu, X.-F. Wu, Y.-C. Zou, and T. Lu, "Early afterglows from radially structured outflows and the application to X-ray shallow decays," *Research in Astronomy and Astrophysics*, vol. 9, no. 8, pp. 911–920, 2009.

[84] Z. L. Uhm, "A semi-analytic formulation for relativistic blast waves with a long-lived reverse shock," *The Astrophysical Journal*, vol. 733, no. 2, article 86, 2011.

[85] Z. L. Uhm, B. Zhang, R. Hascoët, F. Daigne, R. Mochkovitch, and I. H. Park, "Dynamics and afterglow light curves of gamma-ray burst blast waves with a long-lived reverse shock," *The Astrophysical Journal*, vol. 761, no. 2, article 147, 2012.

[86] Z. L. Uhm and B. Zhang, "Dynamics and afterglow light curves of gamma-ray burst blast waves encountering a density bump or void," *The Astrophysical Journal*, vol. 789, no. 1, p. 39, 2014.

[87] Z. G. Dai and T. Lu, "Neutrino afterglows and progenitors of gamma-ray bursts," *The Astrophysical Journal*, vol. 551, no. 1, pp. 249–253, 2001.

[88] Y. Z. Fan, B. Zhang, and D. M. Wei, "Early optical afterglow light curves of neutron-fed gamma-ray bursts," *The Astrophysical Journal*, vol. 628, no. 1, pp. 298–314, 2005.

[89] X. Y. Wang, Z. G. Dai, and T. Lu, "Prompt high-energy gamma-ray emission from the synchrotron self-Compton process in the reverse shocks of gamma-ray bursts," *The Astrophysical Journal Letters*, vol. 546, no. 1, pp. L33–L37, 2001.

[90] X. Y. Wang, Z. G. Dai, and T. Lu, "The inverse Compton emission spectra in the very early afterglows of gamma-ray bursts," *Astrophysical Journal Letters*, vol. 556, no. 2, pp. 1010–1016, 2001.

[91] H. Gao, X. G. Wang, P. Mészáros, and B. Zhang, "A morphological analysis of gamma-ray burst early optical afterglows," *The Astrophysical Journal*. Submitted.

[92] Z. P. Jin and Y. Z. Fan, "GRB 060418 and 060607A: the medium surrounding the progenitor and the weak reverse shock emission," *Monthly Notices of the Royal Astronomical Society*, vol. 378, no. 3, pp. 1043–1048, 2007.

[93] M. V. Medvedev and A. Loeb, "Generation of magnetic fields in the relativistic shock of gamma-ray burst sources," *The Astrophysical Journal*, vol. 526, no. 2, pp. 697–706, 1999.

[94] E. Nakar, T. Piran, and R. Sari, "Pure and loaded fireballs in soft gamma-ray repeater giant flares," *Astrophysical Journal Letters*, vol. 635, no. 1, pp. 516–521, 2005.

[95] S. R. Kulkarni, S. G. Djorgovski, S. C. Odewahn et al., "The afterglow, redshift and extreme energetics of the $\gamma$-ray burst of 23 January 1999," *Nature*, vol. 398, no. 6726, pp. 389–394, 1999.

[96] T. J. Galama, M. S. Briggs, R. A. M. J. Wijers et al., "The effect of magnetic fields on $\gamma$-ray bursts inferred from multi- wavelength

observations of the burst of 23 January 1999," *Nature*, vol. 398, no. 6726, pp. 394–399, 1999.

[97] J. S. Bloom, S. R. Kulkarni, S. G. Djorgovski et al., "The unusual afterglow of the $\gamma$-ray burst of 26 March 1998 as evidence for a supernova connection," *Nature*, vol. 401, no. 6752, pp. 453–456, 1999.

[98] E. E. Fenimore, E. Ramirez-Ruiz, and B. Wu, "GRB 990123: evidence that the gamma rays come from a central engine," *The Astrophysical Journal*, vol. 518, no. 2, pp. L73–L76, 1999.

[99] Z. G. Dai and T. Lu, "The afterglow of GRB 990123 and a dense medium," *Astrophysical Journal Letters*, vol. 519, no. 2, pp. L155–L158, 1999.

[100] S. R. Kulkarni, D. A. Frail, R. Sari et al., "Discovery of a radio flare from GRB 990123," *Astrophysical Journal Letters*, vol. 522, no. 2, pp. L97–L100, 1999.

[101] S. Holland, G. Björnsson, J. Hjorth, and B. Thomsen, "The broken light curves of gamma-ray bursts GRB 990123 and GRB 990510," *Astronomy and Astrophysics*, vol. 364, no. 2, pp. 467–478, 2000.

[102] E. Maiorano, N. Masetti, E. Palazzi et al., "The puzzling case of GRB 990123: multiwavelength afterglow study," *Astronomy and Astrophysics*, vol. 438, no. 3, pp. 821–827, 2005.

[103] A. Corsi, L. Piro, E. Kuulkers et al., "The puzzling case of GRB 990123: prompt emission and broad-band afterglow modeling," *Astronomy & Astrophysics*, vol. 438, no. 3, pp. 829–840, 2005.

[104] A. Panaitescu, "Swift gamma-ray burst afterglows and the forward-shock model," *Monthly Notices of the Royal Astronomical Society*, vol. 379, no. 1, pp. 331–342, 2007.

[105] D. M. Wei, "The GRB early optical flashes from internal shocks: application to GRB 990123, GRB 041219a and GRB 060111b," *Monthly Notices of the Royal Astronomical Society*, vol. 374, no. 2, pp. 525–529, 2007.

[106] D. Lazzati, R. Perna, J. Flasher, V. V. Dwarkadas, and F. Fiore, "Time-resolved spectroscopy of GRB 021004 reveals a clumpy extended wind," *Monthly Notices of the Royal Astronomical Society*, vol. 372, no. 4, pp. 1791–1798, 2006.

[107] W. T. Vestrand, K. Borozdin, D. J. Casperson et al., "RAPTOR: closed-Loop monitoring of the night sky and the earliest optical detection of GRB 021211," *Astronomische Nachrichten*, vol. 325, no. 6–8, pp. 549–552, 2004.

[108] M. C. Nysewander, D. E. Reichart, H. S. Park et al., "Early time chromatic variations in the wind-swept medium of GRB 021211 and the faintness of its afterglow," *The Astrophysical Journal*, vol. 651, no. 2, pp. 994–1004, 2006.

[109] L. Shao and Z. G. Dai, "A reverse-shock model for the early afterglow of GRB 050525A," *The Astrophysical Journal*, vol. 633, no. 2, pp. 1027–1030, 2005.

[110] A. J. Blustin, D. Band, S. Barthelmy et al., "Swift panchromatic observations of the bright gamma-ray burst GRB 050525a," *The Astrophysical Journal*, vol. 637, no. 2, pp. 901–913, 2006.

[111] D. M. Wei, T. Yan, and Y. Z. Fan, "The optical flare and afterglow light curve of GRB 050904 at redshift z = 6.29," *The Astrophysical Journal*, vol. 636, no. 2, pp. L69–L72, 2006.

[112] M. Boër, J. L. Atteia, Y. Damerdji, B. Gendre, A. Klotz, and G. Stratta, "Detection of a very bright optical flare from the gamma-ray burst GRB 050904 at redshift 6.29," *The Astrophysical Journal*, vol. 638, no. 2, pp. L71–L74, 2006.

[113] D. A. Kann, N. Masetti, and S. Klose, "The prompt optical/near-infrared flare of GRB 050904: the most luminous transient ever detected," *Astronomical Journal*, vol. 133, no. 3, pp. 1187–1192, 2007.

[114] L.-J. Gou, D. B. Fox, and P. Mészáros, "Modeling GRB 050904: autopsy of a massive stellar explosion at z = 6.29," *Astrophysical Journal*, vol. 668, no. 2, pp. 1083–1102, 2007.

[115] A. Klotz, B. Gendre, G. Stratta et al., "Continuous optical monitoring during the prompt emission of GRB 060111B," *Astronomy & Astrophysics*, vol. 451, no. 3, pp. L39–L42, 2006.

[116] M. Jelínek, M. Prouza, P. Kubánek et al., "The bright optical flash from GRB 060117," *Astronomy & Astrophysics*, vol. 454, no. 3, pp. L119–L122, 2006.

[117] S. Covino, S. Campana, M. L. Conciatore et al., "Challenging gamma-ray burst models through the broadband dataset of GRB 060908," *Astronomy and Astrophysics*, vol. 521, no. 6, article A53, 2010.

[118] A. Gomboc, S. Kobayashi, C. Guidorzi et al., "Multiwavelength analysis of the intriguing GRB 061126: the reverse shock scenario and magnetization," *Astrophysical Journal*, vol. 687, no. 1, pp. 443–455, 2008.

[119] D. A. Perley, J. S. Bloom, N. R. Butler et al., "The troublesome broadband evolution of GRB 061126: does a gray burst imply gray dust?" *The Astrophysical Journal*, vol. 672, no. 1, pp. 449–464, 2008.

[120] J. L. Racusin, S. V. Karpov, M. Sokolowski et al., "Broadband observations of the naked-eye $\gamma$-ray burst GRB 080319B," *Nature*, vol. 455, no. 7210, pp. 183–188, 2008.

[121] P. Kumar and A. Panaitescu, "What did we learn from gamma-ray burst 080319B?" *Monthly Notices of the Royal Astronomical Society*, vol. 391, no. 1, pp. L19–L23, 2008.

[122] J. S. Bloom, D. A. Perley, W. Li et al., "Observations of the naked-eye GRB 080319B: implications of nature's brightest explosion," *The Astrophysical Journal*, vol. 691, no. 1, pp. 723–737, 2009.

[123] S. B. Pandey, A. J. Castro-Tirado, M. Jelínek et al., "Multi-wavelength observations of the GRB 080319B afterglow and the modeling constraints," *Astronomy and Astrophysics*, vol. 504, no. 1, pp. 45–51, 2009.

[124] Z.-P. Jin, S. Covino, M. Della Valle et al., "GRB 081007 and GRB 090424: the surrounding medium, outflows, and supernovae," *Astrophysical Journal*, vol. 774, no. 2, article 114, 2013.

[125] B. Gendre, A. Klotz, E. Palazzi et al., "Testing gamma-ray burst models with the afterglow of GRB 090102," *Monthly Notices of the Royal Astronomical Society*, vol. 405, no. 4, pp. 2372–2380, 2010.

[126] J. Aleksić, S. Ansoldi, L. A. Antonelli et al., "MAGIC upper limits on the GRB 090102 afterglow," *Monthly Notices of the Royal Astronomical Society*, vol. 437, no. 4, pp. 3103–3111, 2014.

[127] S. B. Pandey, C. A. Swenson, D. A. Perley et al., "GRB 090902B: afterglow observations and implications," *Astrophysical Journal Letters*, vol. 714, no. 1, pp. 799–804, 2010.

[128] R.-Y. Liu and X.-Y. Wang, "Modeling the broadband emission of GRB 090902B," *The Astrophysical Journal*, vol. 730, no. 1, article 1, 2011.

[129] D. Gruber, T. Krühler, S. Foley et al., "Fermi /GBM observations of the ultra-long GRB 091024: a burst with an optical flash," *Astronomy and Astrophysics*, vol. 528, article A15, 2011.

[130] W.-H. Gao, "The physical origin of optical flares following GRB 110205A and the nature of the outflow," *Research in Astronomy and Astrophysics*, vol. 11, no. 11, pp. 1317–1326, 2011.

[131] B. Gendre, J. L. Atteia, M. Boër et al., "GRB 110205A: anatomy of a long gamma-ray burst," *The Astrophysical Journal*, vol. 748, no. 1, article no. 59, 2012.

[132] W. Zheng, R. F. Shen, T. Sakamoto et al., "Panchromatic observations of the textbook GRB 110205A: constraining physical

mechanisms of prompt emission and afterglow," *The Astrophysical Journal*, vol. 751, no. 2, article 90, 2012.

[133] T. Laskar, E. Berger, B. A. Zauderer et al., "A reverse shock in GRB 130427A," *The Astrophysical Journal*, vol. 776, no. 2, article 119, 2013.

[134] A. Panaitescu, W. T. Vestrand, and P. Woźniak, "An external-shock model for gamma-ray burst afterglow 130427A," *Monthly Notices of the Royal Astronomical Society*, vol. 436, no. 4, Article ID stt1792, pp. 3106–3111, 2013.

[135] W. T. Vestrand, J. A. Wren, A. Panaitescu et al., "The bright optical flash and afterglow from the gamma-ray burst GRB 130427A," *Science*, vol. 343, no. 6166, pp. 38–41, 2014.

[136] A. J. van der Horst, Z. Paragi, A. G. de Bruyn et al., "A comprehensive radio view of the extremely bright gamma-ray burst 130427A," *Monthly Notices of the Royal Astronomical Society*, vol. 444, no. 4, pp. 3151–3163, 2014.

[137] R. D. Blandford and R. L. Znajek, "Electromagnetic extraction of energy from Kerr black holes," *Monthly Notices of the Royal Astronomical Society*, vol. 179, no. 3, pp. 433–456, 1977.

[138] S. Kobayashi, T. Piran, and R. Sari, "Hydrodynamics of a relativistic fireball: the complete evolution," *The Astrophysical Journal*, vol. 513, no. 2, pp. 669–678, 1999.

[139] R. Sari, T. Piran, and J. P. Halpern, "Jets in gamma-ray bursts," *Astrophysical Journal Letters*, vol. 519, no. 1, pp. L17–L20, 1999.

[140] Y. Z. Fan, D. M. Wei, and B. Zhang, "$\gamma$-ray burst internal shocks with magnetization," *Monthly Notices of the Royal Astronomical Society*, vol. 354, no. 4, pp. 1031–1039, 2004.

[141] E. V. Derishev and V. V. Kocharovsky, "The neutron component in fireballs of gamma-ray bursts: dynamics and observable imprints," *Astrophysical Journal Letters*, vol. 521, no. 2, pp. 640–649, 1999.

[142] A. M. Beloborodov, "Nuclear composition of gamma-ray burst fireballs," *Astrophysical Journal Letters*, vol. 588, no. 2, pp. 931–944, 2003.

[143] J. Pruet, S. E. Woosley, and R. D. Huffman, "Nucleosynthesis in gamma-ray burst accretion disks," *The Astrophysical Journal*, vol. 586, no. 2, pp. 1254–1261, 2003.

[144] S. Kobayashi, B. Zhang, P. Mészáros, and D. Burrows, "Inverse compton x-ray flare from gamma-ray burst reverse shock," *Astrophysical Journal*, vol. 655, no. 1, pp. 391–395, 2007.

[145] A. M. Beloborodov, "Optical and GeV-TeV flashes from gamma-ray bursts," *Astrophysical Journal Letters*, vol. 618, no. 1, pp. L13–L16, 2005.

[146] S. Horiuchi and S. Ando, "High-energy neutrinos from reverse shocks in choked and successful relativistic jets," *Physical Review D*, vol. 77, no. 6, Article ID 063007, 2008.

[147] M. J. Rees and P. Mészáros, "Refreshed shocks and afterglow longevity in gamma-ray bursts," *Astrophysical Journal Letters*, vol. 496, no. 1, pp. L1–L4, 1998.

[148] R. Sari and P. Mészáros, "Impulsive and varying injection in gamma-ray burst afterglows," *The Astrophysical Journal*, vol. 535, no. 1, pp. L33–L37, 2000.

[149] D. Lazzati and M. C. Begelman, "Thick fireballs and the steep decay in the early X-ray afterglow of gamma-ray bursts," *The Astrophysical Journal*, vol. 641, no. 2, pp. 972–977, 2006.

[150] S. Kobayashi, "Polarization in very early gamma-ray burst afterglow," *International Journal of Modern Physics: Conference Series*, vol. 8, pp. 220–224, 2012.

[151] A. Sagiv, E. Waxman, and A. Loeb, "Probing the magnetic field structure in gamma-ray bursts through dispersive plasma effects on the afterglow polarization," *The Astrophysical Journal*, vol. 615, no. 1, pp. 366–377, 2004.

[152] I. A. Steele, C. G. Mundell, R. J. Smith, S. Kobayashi, and C. Guidorzi, "Ten per cent polarized optical emission from GRB 090102," *Nature*, vol. 462, no. 7274, pp. 767–769, 2009.

[153] C. G. Mundell, I. A. Steels, R. J. Smith et al., "Early optical polarization of a gamma-ray burst afterglow," *Science*, vol. 315, no. 5820, pp. 1822–1824, 2007.

[154] A. Panaitescu, P. Mészáros, and M. J. Rees, "Multiwavelength afterglows in gamma-ray bursts: Refreshed shock and jet effects," *The Astrophysical Journal*, vol. 503, no. 1, pp. 314–324, 1998.

[155] D. Lazzati, E. Rossi, S. Covino, G. Ghisellini, and D. Malesani, "The afterglow of GRB 021004: surfing on density waves," *Astronomy and Astrophysics*, vol. 396, no. 2, pp. L5–L9, 2002.

[156] K. Ioka, S. Kobayashi, and B. Zhang, "Variabilities of gamma-ray burst afterglows: long-acting engine, anisotropic jet, or many fluctuating regions?" *The Astrophysical Journal*, vol. 631, no. 1, pp. 429–434, 2005.

[157] J. Japelj, D. Kopač, S. Kobayashi et al., "Phenomenology of reverse-shock emission in the optical afterglows of gamma-ray bursts," *The Astrophysical Journal*, vol. 785, no. 2, article 84, 2014.

[158] D. A. Perley, A. J. Levan, N. R. Tanvir et al., "A population of massive, luminous galaxies hosting heavily dust-obscured gamma-ray bursts: implications for the use of GRBs as tracers of cosmic star formation," *The Astrophysical Journal*, vol. 778, no. 2, article 128, 2013.

[159] A. De Ugarte Postigo, A. Lundgren, S. Martín et al., "Pre-ALMA observations of GRBs in the mm/submm range," *Astronomy and Astrophysics*, vol. 538, article A44, 2012.

[160] Y. Urata, K. Huang, K. Asada et al., "A new era of sub-millimeter GRB afterglow follow-ups with the Greenland Telescope," http://arxiv.org/abs/1503.07594.

[161] P. Chandra and D. A. Frail, "A radio-selected sample of gamma-ray burst afterglows," *Astrophysical Journal*, vol. 746, no. 2, article 156, 2012.

[162] H. Gao and B. Zhang, "photosphere emission from a hybrid relativistic outflow with arbitrary dimensionless entropy and magnetization in GRBs," *The Astrophysical Journal*, vol. 801, no. 2, article 103, 2015.

[163] J. Paul, J. Wei, S. Basa, and S.-N. Zhang, "The Chinese-French SVOM mission for gamma-ray burst studies," *Comptes Rendus Physique*, vol. 12, no. 3, pp. 298–308, 2011.